

GCWSNet: Generalized Consistent Weighted Sampling for Scalable and Accurate Training of Neural Networks

Ping Li

LinkedIn Ads

700 Bellevue Way NE, Bellevue WA, 98004, USA

pinli@linkedin.com

Weijie Zhao

Rochester Institute of Technology

20 Lomb Memorial Dr, Rochester, NY 14623, USA

wjz@cs.rit.edu

ABSTRACT

We propose using “powered generalized min-max” (pGMM) hashed (linearized) via the “generalized consistent weighted sampling” (GCWS) for training (deep) neural networks (hence the name “GCWSNet”). The pGMM and several related kernels were proposed in 2017 [27]. We demonstrate that pGMM hashed by GCWS provide a numerically stable scheme for applying power transformation on the original data, regardless of the magnitude of p and the data. Our experiments show that GCWSNet often improves the accuracy. It is also evident that GCWSNet converges substantially faster, reaching reasonable accuracy with merely one epoch of the training process. This property is much desired because many applications, such as advertisement click-through rate (CTR) prediction models, or data streams (i.e., data seen only once), often train just one epoch. Another beneficial side effect is that the computations of the first layer of the neural networks become additions instead of multiplications because the input data become binary and highly sparse.

Empirical comparisons with (normalized) random Fourier features (NRFF) are provided. We also propose to reduce the model size of GCWSNet by count-sketch and develop the theory for analyzing the impact of using count-sketch on the accuracy of GCWS. Our analysis shows that an “8-bit” strategy should provide the good trade-off between accuracy and model size. There are other ways to take advantage of GCWS. For example, one can apply GCWS on the last layer to boost the accuracy of trained deep neural nets.¹

CCS CONCEPTS

• **Computing methodologies** → **Machine learning**; • **Theory of computation** → **Theory and algorithms for application domains**; • **Information systems** → **Data management systems**.

KEYWORDS

hashing, neural networks, pGMM kernel, consistent sampling

¹The open-source package <https://github.com/pltrees/GCWSNet> provides the implementation of GCWSNet with multiple deep learning platforms. In particular, the implementation in *paddlepaddle* was conducted while both authors were with the Cognitive Computing Lab, Baidu Research, 10900 NE 8th St. Bellevue, WA 98004, USA.

Permission to make digital or hard copies of all or part of this work for personal or classroom use is granted without fee provided that copies are not made or distributed for profit or commercial advantage and that copies bear this notice and the full citation on the first page. Copyrights for components of this work owned by others than ACM must be honored. Abstracting with credit is permitted. To copy otherwise, or republish, to post on servers or to redistribute to lists, requires prior specific permission and/or a fee. Request permissions from permissions@acm.org.
CIKM '22, October 17–21, 2022, Atlanta, GA, USA

© 2022 Association for Computing Machinery.
ACM ISBN 978-1-4503-9236-5/22/10...\$15.00
<https://doi.org/10.1145/3511808.3557332>

ACM Reference Format:

Ping Li and Weijie Zhao. 2022. GCWSNet: Generalized Consistent Weighted Sampling for Scalable and Accurate Training of Neural Networks. In *Proceedings of the 31st ACM International Conference on Information and Knowledge Management (CIKM '22)*, October 17–21, 2022, Atlanta, GA, USA. ACM, New York, NY, USA, 11 pages. <https://doi.org/10.1145/3511808.3557332>

1 INTRODUCTION

There has been a surge of interest in speeding up the training of large-scale learning algorithms. For example, [51] applied count-sketch type of randomized algorithms [6] to approximate large-scale linear classifiers. [33] applied (b-bit) minwise hashing [3, 4, 28, 30] to approximate the resemblance kernel in high-dimensional binary (0/1) data. In this paper, we propose using the “pGMM” kernel [27] and “generalized consistent weighted sampling” (GCWS) which approximates the pGMM kernel, for training neural networks.

The so-called “generalized min-max” (GMM) kernel was proposed in [26]. For defining the GMM kernel, the first step is a simple transformation on the original data. Consider, for example, the original data vector u_i , $i = 1$ to D . The following transformation, depending on whether an entry u_i is positive or negative,

$$\begin{cases} \tilde{u}_{2i-1} = u_i, & \tilde{u}_{2i} = 0 & \text{if } u_i > 0 \\ \tilde{u}_{2i-1} = 0, & \tilde{u}_{2i} = -u_i & \text{if } u_i \leq 0 \end{cases} \quad (1)$$

converts general data types to non-negative data only. For example, when $D = 2$ and $u = [-3 \ 17]$, the transformed data vector becomes $\tilde{u} = [0 \ 3 \ 17 \ 0]$. The GMM kernel is then defined as follows:

$$GMM(u, v) = \frac{\sum_{i=1}^{2D} \min\{\tilde{u}_i, \tilde{v}_i\}}{\sum_{i=1}^{2D} \max\{\tilde{u}_i, \tilde{v}_i\}}. \quad (2)$$

Note that, the GMM kernel in (2) still has no tuning parameter, unlike (e.g.) the popular Gaussian (RBF) kernel. A simple strategy to introduce tuning parameters is the so-called “pGMM” kernel [27]:

$$pGMM(u, v; p) = \frac{\sum_{i=1}^{2D} (\min\{\tilde{u}_i, \tilde{v}_i\})^p}{\sum_{i=1}^{2D} (\max\{\tilde{u}_i, \tilde{v}_i\})^p}, \quad (3)$$

where $p \in \mathbb{R}$ is a tuning parameter. Note that this is mathematically equivalent to first applying a power transformation on the data (\tilde{u}, \tilde{v}) before computing the GMM kernel. It will soon be clear that, combined with GCWS hashing, pGMM provides a numerically highly stable scheme for applying the power transformation.

1.1 Kernel SVM Experiments

While our focus is on training neural networks, we nevertheless provide a set of experimental studies on kernel SVMs for evaluating the pGMM kernel as in (3), in comparison with the linear kernel and the (best-tuned) RBF (Gaussian) kernel, as reported in Table 1.

Table 1: Public datasets and l_2 -regularized kernel SVM results. We report test accuracies for the linear kernel, the best-tuned RBF kernel, the (tuning-free) GMM kernel, and the best-tuned pGMM kernel, at their individually-best SVM regularization C values. The results on linear kernels were obtained by LIBLINEAR [11] and the kernel SVM experiments were conducted using LIBSVM and pre-computed kernel matrices. The datasets are from the UCI repository, except for M-Noise1 and M-Image used by [22, 24, 27, 34] for testing deep learning algorithms and boosted trees. <https://hunch.net/?p=1467>

Dataset	# train, # test, # dim	linear	RBF	GMM	pGMM (p)
SEMG	1800, 1800, 2500	19.3	29.0	54.0	56.1 (2)
DailySports	4560, 4560, 5625	77.7	97.6	99.6	99.6 (0.6)
M-Noise1	10000, 4000, 784	60.3	66.8	71.4	85.2 (80)
M-Image	12000, 50000, 784	70.7	77.8	80.9	89.5 (50)
PAMAP101	188209, 188208, 51	75.3	—	—	—
Covtype	290506, 290506, 54	71.5	—	—	—

For the SEMG dataset, the accuracies for the linear kernel and the (best-tuned) RBF kernel are very low, i.e., 19.3% and 29.0%, respectively. Perhaps surprisingly, the GMM kernel reaches 54% (with no tuning parameter) and the pGMM kernel achieves an accuracy of 56.1% at $p = 2$. For the M-Noise1 dataset, the best power parameter is $p = 80$ with an accuracy of 85.2%. Readers can check out the deep learning experiments reported in [22] and confirm that they are inferior to the pGMM kernel, for the M-Noise1 dataset.

It is not at all our intention to debate which type of classifiers work the best. We believe the performance highly depends on the datasets. Nevertheless, we hope that it is clear from Table 1 that the pGMM kernel is able to achieve comparable or better accuracy than the RBF kernel on a wide range of datasets. Note that, there are more than 10 datasets used in [22, 24], such as M-Noise2, ..., M-Noise6, etc which exhibit similar behaviors as M-Noise1.

1.2 Linearizing pGMM Kernel via Generalized Consistent Weighted Sampling

When using LIBSVM pre-computed kernel functionality, we find it is rather difficult if the number of training examples exceeds merely 30,000. It has been a well-known challenging task to scale up kernel learning for large datasets [2]. This has motivated many studies on approximating (linearizing) nonlinear kernels. In this paper, we adopt the “generalized consistent weighted sampling” (GCWS) to approximate the pGMM kernel, in the context of training neural networks for any tuning parameter p , as illustrated in Algorithm 1.

Algorithm 1 Generalized consistent weighted sampling (GCWS) for hashing the pGMM kernel.

Input: Data vector u_i ($i = 1$ to D)

Generate vector \tilde{u} in $2D$ -dim by (1).

for i from 1 to $2D$ **do**

$r_i \sim \text{Gamma}(2, 1)$, $c_i \sim \text{Gamma}(2, 1)$, $\beta_i \sim \text{Uniform}(0, 1)$

$t_i \leftarrow \lfloor p \frac{\log \tilde{u}_i}{r_i} + \beta_i \rfloor$, $a_i \leftarrow \log(c_i) - r_i(t_i + 1 - \beta_i)$

end for

Output: $i^* \leftarrow \arg \min_i a_i$, $t^* \leftarrow t_{i^*}$

Algorithm 1 uses vector u for the illustration. Given another vector v , we feed it to GCWS using the same set of random numbers: r_i , c_i , β_i . For differentiation, we name the hash samples as (i_u^*, t_u^*) and (i_v^*, t_v^*) . We first present the basic probability result as a theorem.

THEOREM 1.

$$P[(i_u^*, t_u^*) = (i_v^*, t_v^*)] = pGMM(u, v). \quad (4)$$

The proof of Theorem 1 directly follows from the basic theory of consistent weighted sampling (CWS) [18, 31, 37]. Although the original CWS algorithm is designed (and proved) only for non-negative data, we can see that the two transformations, i.e., converting general data types to non-negative data by (1) and applying the power on the converted data as in (3), are only pre-processing steps and the same proof for CWS will go through for GCWS.

Note that, in Algorithm 1, while the value of the output i^* is upper bounded by $2D$, the other integer output t^* is unbounded. This makes it less convenient for the implementation. The next Theorem provides the basis for the (b-bit) implementation of GCWS.

THEOREM 2. Assume that we can map (i_u^*, t_u^*) uniformly to a space of b bits denoted by $(i_u^*, t_u^*)_b$. Similarly, we have $(i_v^*, t_v^*)_b$. Then

$$P[(i_u^*, t_u^*)_b = (i_v^*, t_v^*)_b] = pGMM(u, v) + \frac{1}{2^b} \{1 - pGMM(u, v)\}. \quad (5)$$

1.3 Practical Implementation of GCWS

For each input data vector, we need to generate k hash values, for example, $(i_{u,j}^*, t_{u,j}^*)$, $j = 1$ to k , for data vector u . The mapping of $(i_{u,j}^*, t_{u,j}^*)$ uniformly to $(i_{u,j}^*, t_{u,j}^*)_b$ is actually not a trivial task, in part because t^* is unbounded. Based on the intensive experimental results in [25] (for the original CWS algorithm), we will take advantage of following approximation:

$$P[i_u^* = i_v^*] \approx P[(i_u^*, t_u^*) = (i_v^*, t_v^*)] = pGMM(u, v). \quad (6)$$

and only keep the lowest b bits of i^* (unless we specify otherwise).

Suppose that, for data vector u , we obtain $k = 3$ hash values which, using only the lowest $b = 2$ bits, become $(3, 0, 1)$. We then concatenate their “one-hot” representation $[1\ 0\ 0\ 0\ 0\ 0\ 1\ 0\ 0\ 1\ 0]$ and feed it to subsequent tasks for classification, regression, or clustering. In other words, with k hashes and b bits, for each input vector we obtain a binary vector of length $2^b \times k$ with exactly k 1’s.

The approximation in (6) (so called “0-bit” CWS) was purely an empirical (and mysterious) observation by [25]. Recently, [31] has partially resolved the mystery by developing a closely-related (but different) hashing method based on extremal processes.

1.4 History of Consistent Weighted Sampling

For binary (0/1) data, the pGMM kernel becomes the resemblance (Jaccard) similarity and GCWS is essentially equivalent to the celebrated minwise hashing algorithm [3, 4, 28, 30], with numerous applications [1, 5, 8–10, 13–15, 17, 19, 23, 33, 38–42, 45, 47–50, 54].

There exist strategies for generalizing the resemblance and minwise hashing for non-binary data. For example, CRS (Conditional Random Sampling) [28, 29] stores the smallest (bottom) k non-zero entries for each row of the data matrix, after one (and only one) random permutation on the columns. CWS (consistent weighted sampling) is another strategy, originally for non-negative data.

The development of consistent weighted sampling (CWS) algorithm in its current form was due to [18, 37], as well as the earlier versions such as [16]. [25] made the observation about the “0-bit” CWS, i.e., (6) and applied it to approximate large-scale kernel machines using linear algorithms. [26] generalized CWS to general data types which can have negative entries and demonstrated the considerable advantage of CWS over random Fourier features [43]. From the computational perspective, CWS and variants such as [31] are efficient in sparse data. For dense data, algorithms based on rejection sampling [7, 21, 36, 46] can be much more efficient than CWS. For relatively high-dimensional datasets, the method of “bin-wise CWS” (BCWS) [32] would always be recommended. Simply speaking, the basic idea of BCWS is to divide the data matrix into bins and then apply CWS (for sparse data) or rejection sampling (for dense data) in each bin. Finally, we should add that, despite the work [31], the mathematical explanation of the “0-bit” approximation (6), empirically observed by [25], remains an open problem.

1.5 Our Contributions

We develop GCWS (generalized CWS) for hashing the pGMM kernel and then apply GCWS for efficiently training neural networks. We name our procedure GCWSNet and show that GCWSNet can often achieve more accurate results compared with the standard neural networks. We also observe that the convergent speed of GCWSNet can be substantially faster than the standard neural networks. In fact, GCWS typically achieves a reasonable accuracy in (less than) one epoch. This property might be a huge advantage. For example, in many applications such as data streams, one of the 10 challenges in data mining [52], each sample vector is only seen once and hence only one epoch is allowed in the training process. In commercial search engines, when training click-through rate (CTR) deep learning models, typically only one epoch is used [12, 53] as the training data size is on the petabyte scale and new observations (i.e., user clicks) keep arriving at a very fast rate. Additionally, there is a side benefit of GCWSNet, because the computations at the first layer become additions instead of multiplications.

2 GCWSNET

For each input data vector, we first generate k hash values (i^* , t^*) using GCWS as in Algorithm 1. We adopt the “0-bit” approximation (6) and keep only the lowest b bits of i^* . For example, suppose $k = 3$, $b = 2$ bits, and the hash values become (3, 0, 1). We concatenate their “one-hot” representations to obtain [1 0 0 0 0 0 1 0 0 1 0], which is the input data fed to neural networks. In short, with k hashes and b bits, for each input data vector we obtain a binary vector of length $2^b \times k$ with exactly k 1’s.

In the experiments, we adopted the Adam optimizer [20] and set the initial learning rate to be 0.001. We use “ReLU” for the activation function; other learning rates gave either similar or worse results in our experiments. The batch size was set to be 32 for all datasets except Covtype for which we use 128 as the batch size. We report experiments for neural nets with no hidden units (denoted by “ $L = 1$ ”), one layer of H hidden units (denoted by “ $L = 2$ ”) and two layers (denoted by “ $L = 3$ ”) of hidden units (H units in the first hidden layer and $H/2$ units in the second hidden layer). We have also experimented with more layers.

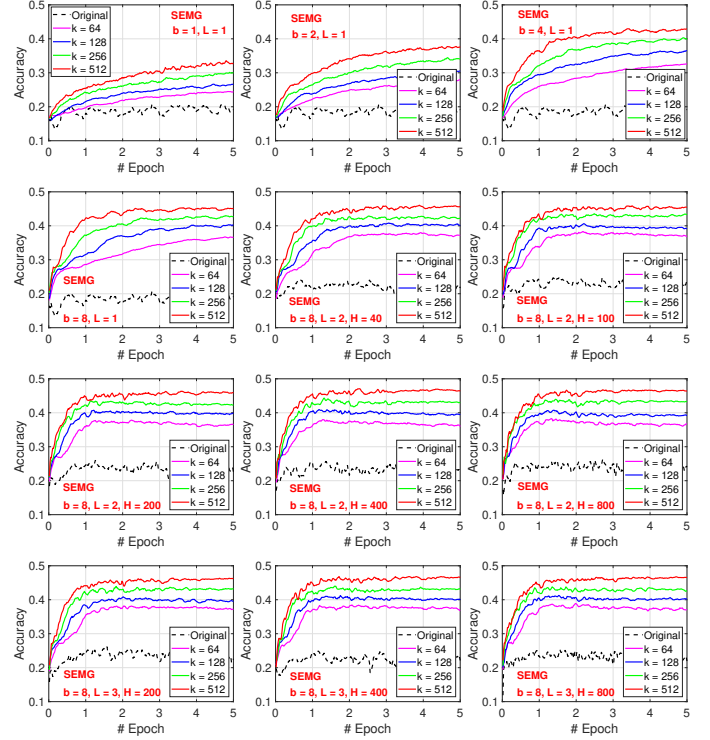


Figure 1: GCWSNet with $p = 1$, for $b \in \{1, 2, 4, 8\}$ and $k \in \{64, 128, 256, 512\}$, on the SEMG dataset (see Table 1). We report the test accuracy for 5 epochs. “ $L = 1$ ” means no hidden units, i.e., just logistic regression. “ $L = 2$ ” means one hidden layer of H units. “ $L = 3$ ” means two hidden layers with H units in the first hidden layer and $H/2$ units in the second hidden layer. The results for the original data (dashed black curves) are much worse than GCWSNet, as expected from Table 1. One important observation is that GCWSNet converges fast, reaching a good accuracy after just one epoch of training.

Figure 1 presents the results on the SEMG dataset using GCWS (with $p = 1$) along with the results on the original data (dashed black curves). This is a small dataset with 2,500 features. The dashed (black) curves for $L = 1$ (i.e., neural nets with no hidden units) are consistent with the results in Table 1, i.e., an accuracy of $< 20\%$ for linear classifier. Using one layer of H hidden units (i.e., $L = 2$) improves the accuracy noticeably (to $\approx 25\%$). Using two layers of hidden units (i.e., $L = 3$) further improves the accuracy only little.

For the SEMG dataset, GCWS is highly effective. We report the experiments for $b \in \{1, 2, 4, 8\}$ and $k \in \{64, 128, 256, 512\}$. The cost of training SGD is largely determined by the number of nonzero entries. Note that even with $k = 512$, the number of nonzero entries in each input training data vector is only $k = 512$ while the original SEMG dataset has 2,500 nonzero entries in each data vector.

We recommend using a large b value as long as the model can be stored. With $b = 8$ bits, GCWSNet converges fast and typically reaches a reasonable accuracy after one epoch (i.e., all the training samples have been used exactly once). This property can be highly beneficial for applications in (e.g.,) data streams or training CTR models for commercial search engines [12, 53].

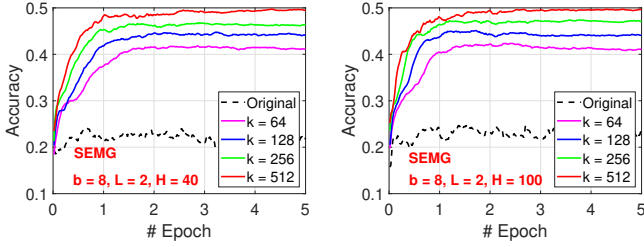


Figure 2: GCWSNet with $p = 2$ on the SEMG dataset. Note that for the original data (dashed black curves), we still report the original results without applying the power transformation. The results on original data with power transformation using $p = 2$ are actually not too much different from using $p = 1$.

Table 1 shows that, for the SEMG dataset, the pGMM kernel with $p = 2$ improves the classification accuracy. Thus, we also report the results of GCWSNet for $p = 2$ in Figure 2. Compared with Figure 1, the improvements are obvious. Figure 2 also again confirms that training just one epoch can already reach good accuracies.

Next we examine the experimental results on the Covtype dataset, in Figure 3 for 100 epochs. Again, we can see that GCWSNet converges substantially faster. To better view the convergence, we

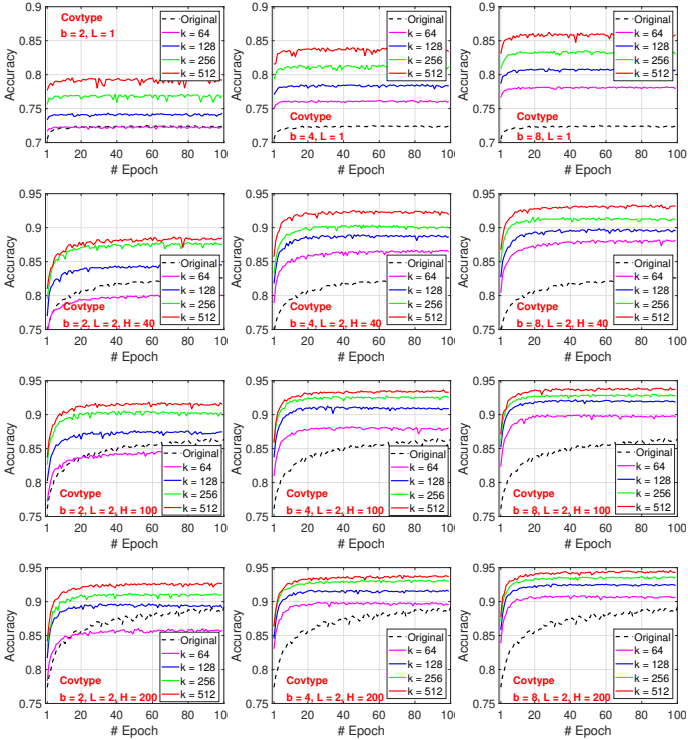


Figure 3: GCWSNet with $p = 1$, for $b \in \{2, 4, 8\}$ and $k \in \{64, 128, 256, 512\}$, on the Covtype dataset, for 100 epochs. The results for the original data are reported as dashed (black) curves, which are substantially worse than the results of GCWSNet. Again, GCWSNet converges much faster than training on the original data.

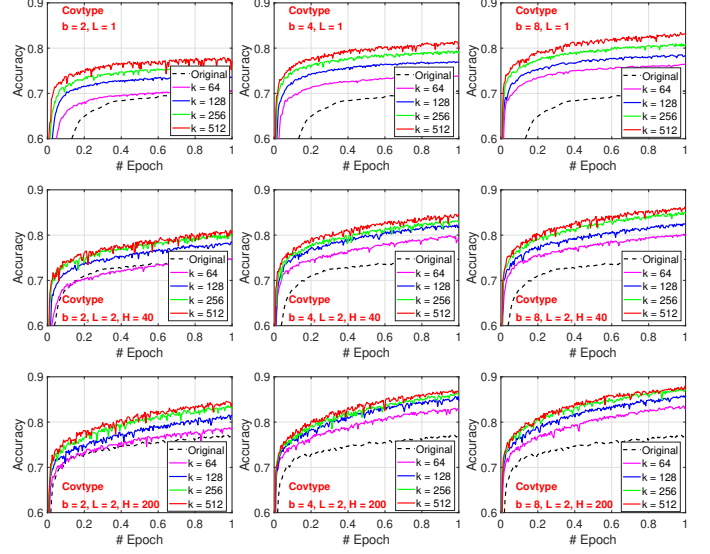


Figure 4: GCWSNet with $p = 1$, for $b \in \{2, 4, 8\}$ and $k \in \{64, 128, 256, 512\}$, on the Covtype dataset, for just one epoch, to illustrate that GCWSNet converges much faster.

repeat the same plots in Figure 4 but for just 1 epoch. As the Covtype dataset has 290,506 training samples, we cannot compute the pGMM kernel directly. LIBLINEAR reports an accuracy of 71.5%, which is consistent with the results for $L = 1$ (i.e., no hidden layer).

The experiments on the Covtype dataset reveal a practically important issue, if applications only allow training for one epoch, even though training more epochs might lead to noticeably better accuracies. For example, consider the plots in the right-bottom corner in both Figure 3 and Figure 4, for $b = 8, L = 2, H = 200$. For the original data, if we stop after one epoch, the accuracy would drop from about 89% to 77%, corresponding to a 13.5% drop of accuracy. However, for GCWSNet with $k = 64$, if the training stops after one epoch, the accuracy would drop from 91% to just 84% (i.e., a 7.7% drop). This again confirms the benefits of GCWSNet in the scenario of one-epoch training.

Figure 5 reports the summary of the test accuracy for Covtype and just one epoch, to better illustrate the impact of b, H, k , and L .

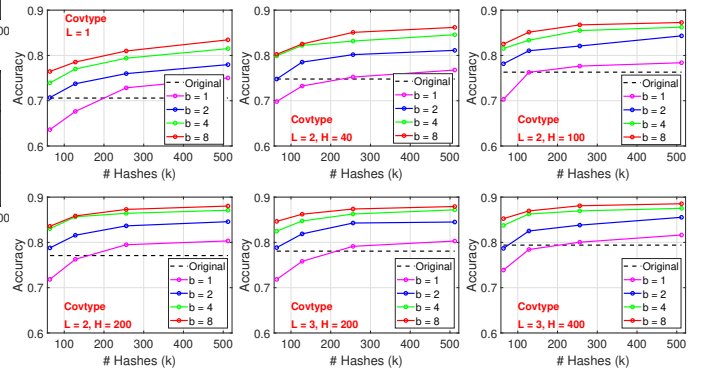


Figure 5: Summary results of GCWSNet with $p = 1$ on the Covtype dataset, at the end of the first epoch.

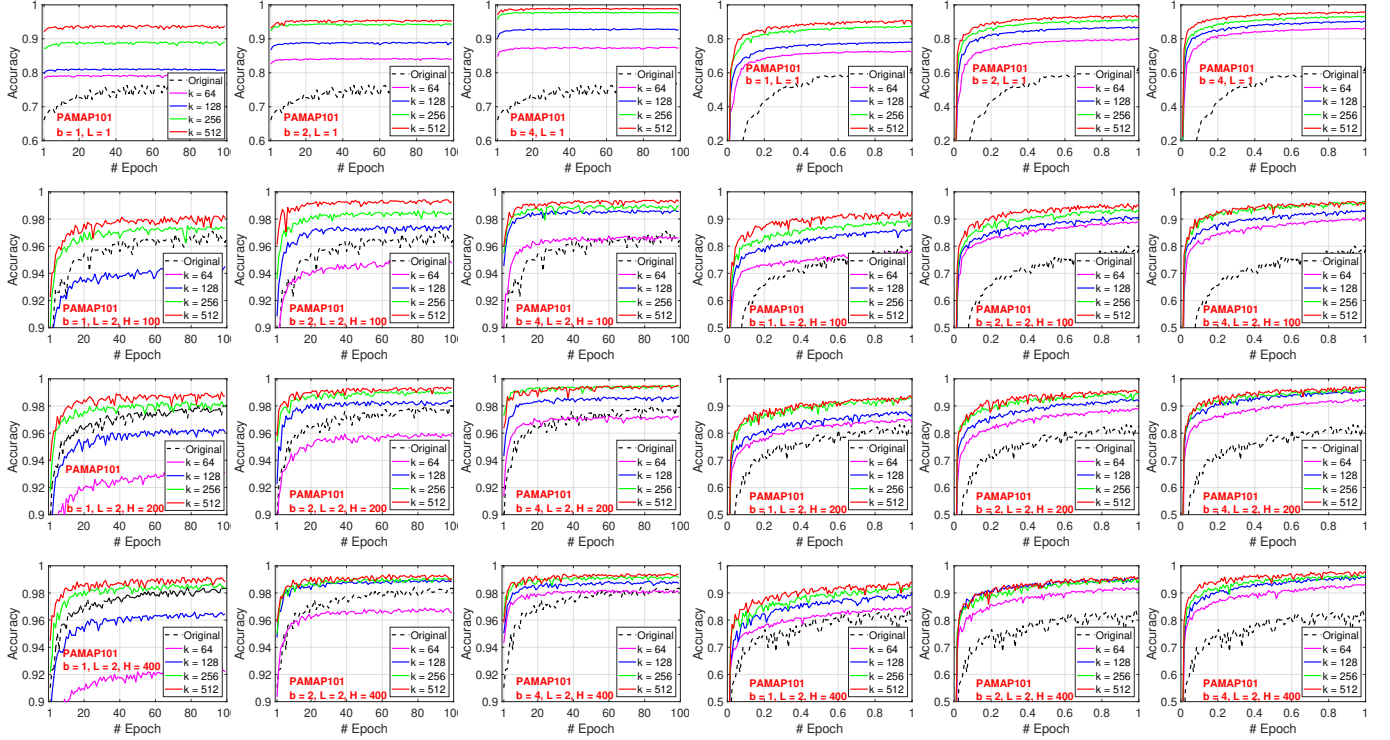


Figure 6: GCWSNet with $p = 1$, for $b \in \{1, 2, 4\}$ and $k \in \{64, 128, 256, 512\}$, on the PAMAP101 dataset, for 100 epochs. Again, we can see that GCWSNet converges much faster than training on the original data.

Next, Figure 6 and Figure 7 present the experimental results on the PAMAP101 dataset, for We report the results for 100 epochs in Figure 6 and the results for just 1 epoch in Figure 7. Again, we can see that GCWSNet converges much faster and can reach a reasonable accuracy even with only one epoch of training.

Finally, we summarize the results on the DailySports dataset, the M-Noise1 dataset, and the M-Image dataset, in Figure 8, Figure 9, and Figure 10, respectively, for just 1 epoch. For DailySports, we let $p = 1$. For M-Noise1 and M-Image, we use $p = 80$ and $p = 50$, respectively, as suggested in Table 1.

3 COMBINING GCWS WITH COUNT-SKETCH

GCWS generates high-dimensional binary sparse inputs. With k hashes and b bits for encoding each hashed value, we obtain a vector of size $2^b \times k$ with exactly k 1's, for each original data vector. While the (online) training cost is mainly determined by k the number of nonzero entries, the model size is still proportional to $2^b \times k$. This might be an issue for the GPU memory when both k and b are large. In this scenario, the well-known method of “count-sketch” might be helpful for reducing the model size.

Count-sketch [6] was originally developed for recovering sparse signals (e.g., “elephants” or “heavy hitters” in network/database terminology). [51] applied count-sketch as a dimension reduction tool. The key step is to independently and uniformly hash elements of the data vectors to buckets $\in \{1, 2, 3, \dots, B\}$ and the hashed value is the weighted sum of the elements in the bucket, where the weights are

Figure 7: GCWSNet with $p = 1$, for $b \in \{1, 2, 4\}$ and $k \in \{64, 128, 256, 512\}$, on the PAMAP101 dataset, just for 1 epoch. Again, we can see that GCWSNet converges much faster than training on the original data.

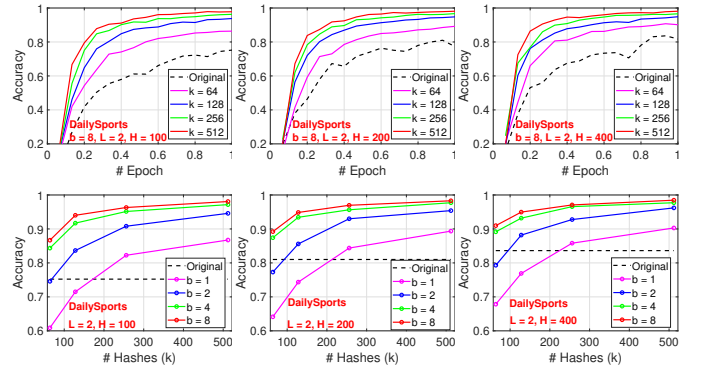


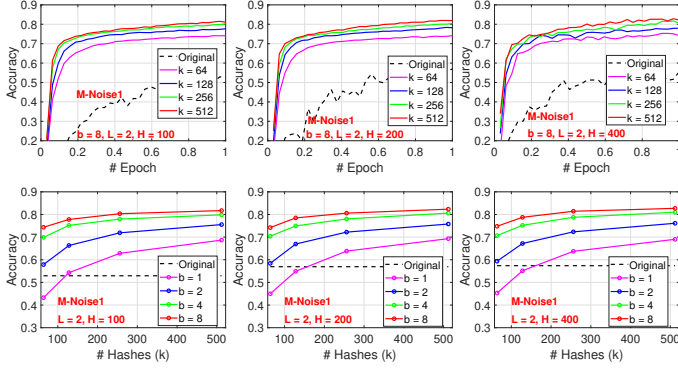
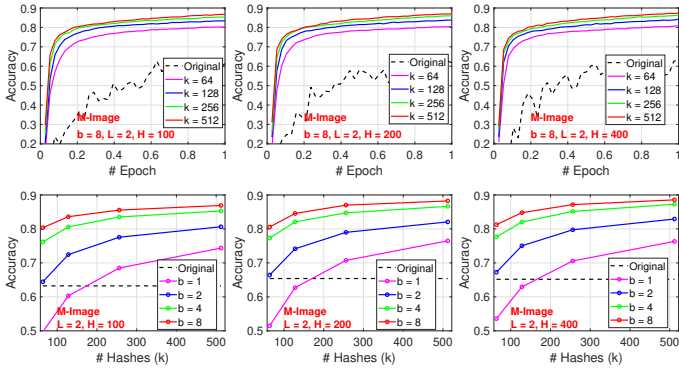
Figure 8: GCWSNet with $p = 1$ on DailySports, for one epoch.

generated from a random distribution which must be $\{-1, 1\}$ with equal probability (the reason will soon be clear). That is, we have $h(i) = j$ with probability $\frac{1}{B}$, where $j \in \{1, 2, \dots, B\}$. For convenience, we introduce an indicator function:

$$I_{ij} = \begin{cases} 1 & \text{if } h(i) = j \\ 0 & \text{otherwise} \end{cases}$$

Consider two vectors $x, y \in \mathbb{R}^d$ and assume d is divisible by B , without loss of generality. We also generate a random vector r_i , $i = 1$ to d , i.i.d., with the following property:

$$E(r_i) = 0, \quad E(r_i^2) = 1, \quad E(r_i^3) = 0, \quad E(r_i^4) = s \quad (7)$$

Figure 9: GCWSNet with $p = 80$ on M-Noise1, for one epoch.Figure 10: GCWSNet with $p = 50$ on M-Image, for one epoch.

Then we generate k (count-sketch) hashed values for x and y :

$$z_j = \sum_{i=1}^d x_i r_i I_{ij}, \quad w_j = \sum_{i=1}^d y_i r_i I_{ij}, \quad j = 1, 2, \dots, B \quad (8)$$

The following Theorem 3 says that the inner product $\langle z, w \rangle = \sum_{j=1}^B z_j w_j$ is an unbiased estimator of $\langle x, y \rangle$.

THEOREM 3. [33]

$$E\{\langle z, w \rangle\} = \langle x, y \rangle = \sum_{i=1}^d x_i y_i, \quad (9)$$

$$\begin{aligned} \text{Var}\{\langle z, w \rangle\} &= (s-1) \sum_{i=1}^d x_i^2 y_i^2 \\ &+ \frac{1}{B} \left[\sum_{i=1}^d x_i^2 \sum_{i=1}^d y_i^2 + \left(\sum_{i=1}^d x_i y_i \right)^2 - 2 \sum_{i=1}^d x_i^2 y_i^2 \right]. \end{aligned} \quad (10)$$

The above theorem implies that we must have $E(r_i^4) = s = 1$. There is only one such distribution, i.e., $\{-1, +1\}$ with equal probability.

Now we are ready to present our idea of combining GCWS with count-sketch. Recall that in the ideal scenario, we map the output of GCWS (i^*, t^*) uniformly to a b -bit space of size 2^b , denoted by $(i^*, t^*)_b$. For the original data vector u , we generate k such (integer) hash values, denoted by $(i_{u,j}^*, t_{u,j}^*)_b$, $j = 1$ to k . Then we concatenate the k one-hot representations of $(i_{u,j}^*, t_{u,j}^*)_b$, we obtain a binary vector of size $d = 2^b \times k$ with exactly k 1's. Similarly, we

have $(i_{v,j}^*, t_{v,j}^*)_b$, $j = 1$ to k and the corresponding binary vector of length $2^b \times k$. Once we have the sparse binary vectors, we can apply count-sketch with B bins. For convenience, we denote

$$B = (2^b \times k)/m. \quad (11)$$

That is, m represents the dimension reduction factor, and $m = 1$ means no reduction. We can then generate the $(B\text{-bin})$ count-sketch samples, z and w , as in (8). We present the theoretical results on the inner product $\langle z, w \rangle$ as the next theorem, in a way that its proof should be self-explanatory.

THEOREM 4. Consider original data vector u and v . Denote $P_b = P\{(i_{u,j}^*, t_{u,j}^*)_b = (i_{v,j}^*, t_{v,j}^*)_b\}$. Vector z of size B is the $(B\text{-bin})$ count-sketch samples generated from the concatenated binary vector from the one-hot representation of $(i_{u,j}^*, t_{u,j}^*)_b$. Similarly, w of size B is the count-sketch samples for v . Also, denote

$$a = \sum_{j=1}^k 1\{(i_{u,j}^*, t_{u,j}^*)_b = (i_{v,j}^*, t_{v,j}^*)_b\}. \quad (12)$$

Conditioning on the GCWS output $(i_{u,j}^*, t_{u,j}^*)_b, (i_{v,j}^*, t_{v,j}^*)_b$ and using Theorem 3 with $s = 1$, we have

$$E\{\langle z, w \rangle | \text{GCWS}\} = a, \quad (13)$$

$$\text{Var}\{\langle z, w \rangle | \text{GCWS}\} = \frac{1}{B} [k^2 + a^2 - 2a]. \quad (14)$$

Note that a is binomial $\text{Bin}(k, P_b)$, i.e., $E(a) = kP_b$, $\text{Var}(a) = kP_b(1 - P_b)$. Therefore, unconditionally, we have

$$E\{\langle z, w \rangle\} = kP_b, \quad (15)$$

$$\text{Var}\{\langle z, w \rangle\} = \frac{1}{B} [k^2 + k^2 P_b^2 - kP_b^2 - kP_b] + kP_b(1 - P_b). \quad (16)$$

Define the estimator \hat{P}_b as

$$\hat{P}_b = \frac{\langle z, w \rangle}{k}. \quad (17)$$

Then

$$E(\hat{P}_b) = P_b, \quad (18)$$

$$\text{Var}(\hat{P}_b) = \frac{P_b(1 - P_b)}{k} + \frac{1}{B} [1 + P_b^2 - P_b^2/k - P_b/k]. \quad (19)$$

In the above Theorem, the variance $\text{Var}(\hat{P}_b)$ (19) in Theorem 4 has two parts. The first term $\frac{P_b(1 - P_b)}{k}$ is the usual variance without using count-sketch. The second term $\frac{1}{B} [1 + P_b^2 - P_b^2/k - P_b/k]$ represents the additional variance due to count-sketch. The hope is that the additional variance would not be too large, compared with $\frac{P_b(1 - P_b)}{k}$. Let $B = (2^b \times k)/m$, then the second term can be written as $\frac{1}{k} \frac{m}{2^b} [1 + P_b^2 - P_b^2/k - P_b/k]$. To assess the impact of count-sketch, we need to compare $P_b(1 - P_b)$ with $\frac{m}{2^b} [1 + P_b^2 - P_b^2/k - P_b/k]$, which is approximately $\frac{m}{2^b} [1 + P_b^2]$, as k has to be sufficiently large. Recall from Theorem 2 $P_b = J + \frac{1}{2^b}(1 - J)$, where $J =$

$pGMM(u, v; p) = \frac{\sum_{i=1}^{2D} (\min\{\tilde{u}_i, \tilde{v}_i\})^p}{\sum_{i=1}^{2D} (\max\{\tilde{u}_i, \tilde{v}_i\})^p}$. We can hence resort to the following “ratio” to assess the impact of count-sketch on the variance:

$$R = R(b, J, m) = \frac{m}{2^b} \frac{1 + P_b^2}{P_b(1 - P_b)}, \text{ where } P_b = J + \frac{1}{2^b}(1 - J). \quad (20)$$

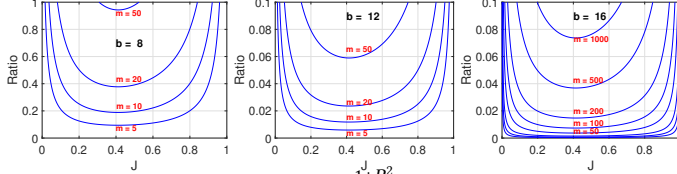


Figure 11: The ratio (20) $R = \frac{m}{2^b} \frac{1+P_b^2}{P_b(1-P_b)}$, where $P_b = J + \frac{1}{2^b}(1-J)$ and J the pGMM similarity of interest, for $b \in \{8, 12, 16\}$ and a series of m values. Ideally, we would like to see large m and small ratio values.

As shown in Figure 11, when $b = 16$, the ratio is small even for $m = 1000$. However, when $b = 8$, the ratio is not too small after $m > 10$; and hence we should only expect a saving by an order magnitude if $b = 8$ is used. The choice of b has, to a good extent, to do with D , the original data dimension. When the data are extremely high-dimensional, say $D = 2^{30}$, we expect an excellent storage savings can be achieved by using a large b and a large m .

For practical consideration, we consider two strategies for choosing m , as illustrated in Figure 12. The first strategy (left panel) is “always using half of the bits”, that is, we let $m = 2^{b/2}$. This method is probably a bit conservative for $b \geq 16$. The second strategy (right panel) is “always using 8 bits” which corresponds to almost like a single curve, because $R = \frac{1}{2^8} \frac{1+P_b^2}{P_b(1-P_b)}$ in this case and $P_b = J + (1-J)\frac{1}{2^b} \approx J$ when $b \geq 8$.

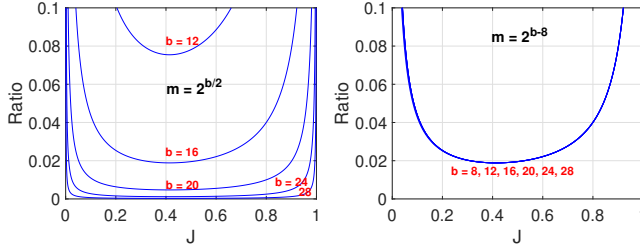


Figure 12: The ratio (20) for two strategies of choosing m . Left panel: we let $m = 2^{b/2}$ (i.e., always using half of the bits). Right panel: for $b \geq 8$ we let $m = 2^{b-8}$ (i.e., always use 8 bits).

We believe the “always using 8 bits” strategy might be a good practice. In implementation, it is convenient to use 8 bits (i.e., one byte). Even when we really just need 5 or 6 bits, we might as well simply use one byte to avoid the trouble of performing bits-packing.

We conclude this section by providing an empirical study on M-Noise1 and M-Image and summarize the results in Figure 13. For both datasets, when $m \leq 16$, we do not see an obvious drop of accuracy, compared with $m = 1$ (i.e., without using count-sketch). This confirms the effectiveness of our proposed procedure by combining GCWSNet with count-sketch.

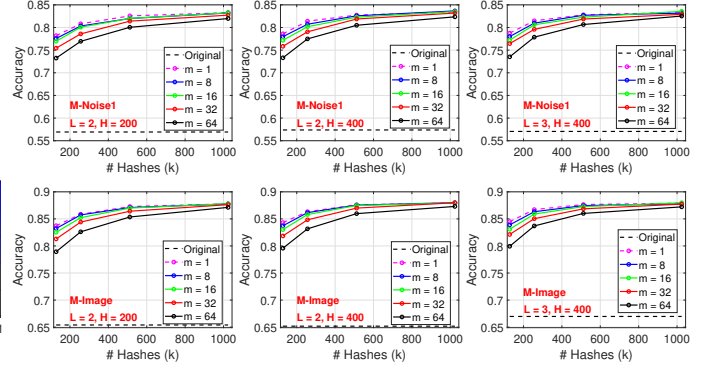


Figure 13: GCWS combined with count-sketch for reducing the model size by a factor of m , where $m = (2^b \times k)/B$ and B is the number of bins in the count-sketch step. $m = 1$ means there is no reduction. We can see that at least with $m = 8$ or $m = 16$, there is no obvious loss of accuracy.

4 ROBUST POWER TRANSFORMATION

In Algorithm 1, this step (on nonzero entries)

$$t_i \leftarrow \left\lfloor p \frac{\log \tilde{u}_i}{r_i} + \beta_i \right\rfloor \quad (21)$$

suggests that GCWS can be viewed as a robust power transformation on the data. It should be clear that GCWS is not simply taking the log-transformation on the original data. We compare three different strategies for data preprocessing. (i) GCWS; (ii) feeding the power transformed data (e.g., u^p) to neural nets; (iii) feeding the log-power transformed data (e.g., $p \log u$) to neural nets.

Naively applying power transformation on the original data might encounter practical problems. For example, when data entries contain large values such as “1533” or “396”, applying a powerful transformation such as $p = 80$ might lead to overflow problems and other issues such as loss of accuracy during computations. Using the log-power transformation, i.e., $p \times \log u$, should alleviate many problems but new issues might arise. For example, when data entries (u) are small. How to handle zeros is another headache with log-power transformation.

Here, we provide an experimental study on the UCI Pendigits dataset, which contains positive integers features (and many zeros). The first a few entries of the training dataset are “8 1:47 2:100 3:27 4:81 5:57 6:37 7:26 10:23 11:56” (in LIBSVM format). As shown in Figure 14, after $p \geq 15$, directly applying the power transformation (i.e., u^p) makes the training fail. The log-transformation (i.e., $p \log u$) seems to be quite robust in this dataset, because we use a trick by letting $p \log 0 = 0$, which seems to work well for this dataset. On the other hand, GCWS with any p produces reasonable predictions, although it appears that $p \in [0.5, 5]$ (a wide range) is the optimal range for GCWSNet. The experiments on Pendigits confirm the robustness of GCWSNet with any p . Additionally, the experiments once again verify that GCWSNet converges really fast and achieves a reasonable accuracy as early as in 0.1 epoch.

Next, we present the experiments on the M-Noise1 dataset, which is quite different from the Pendigits dataset. The first a few entries are “3 1:0.82962122 2:0.56410292 3:0.27904908 4:0.25310652 5:0.29387237” (also in LIBSVM format). This dataset is actually

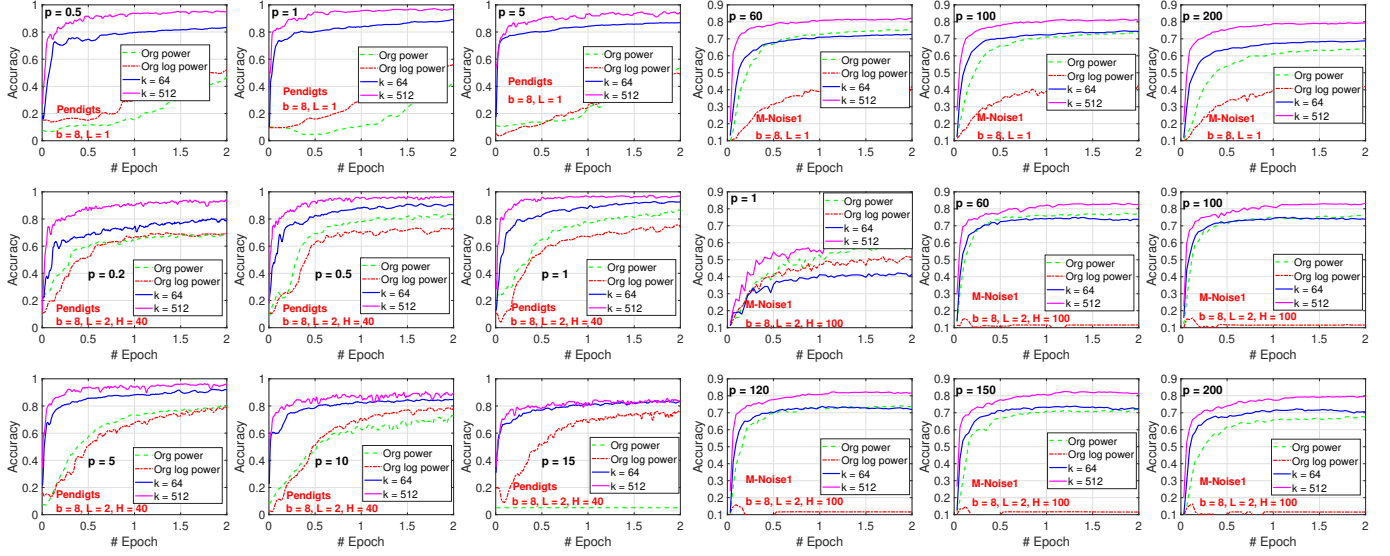


Figure 14: GCWS with a wide range of p values, on the UCI Pendigits dataset, for $b = 8$ and $k \in \{64, 512\}$. We can see that using $p \in [0.5, 5]$ produces the best results. Also, the results of GCWSNet are still reasonable even with very large or very small p values. In comparison, we apply the power transformation (i.e., u^p) and log-power transformation (i.e., $p \log u$, treating $u \log 0 = 0$) on the original data and feed the transformed data directly to neural nets. Their results are not as accurate compared with GCWSNet. Also, the power transformation encountered numerical issues with $p \geq 15$.

dense, with (almost) no zero entries. As shown in Figure 15, using the log-power transformation produced very bad results, except for p close 1. Directly applying the power transformation seems to work well on this dataset (unlike Pendigits), although we can see that GCWSNet still produces more accurate predictions.

To conclude this section, we should emphasize that we do not claim that we have fully solved the data preprocessing problem, which is a highly crucial task for practical applications. We simply introduce GCWSNet with one single tuning parameter which happens to be quite robust, in comparison with obvious (and commonly used) alternatives for power transformations.

5 USING BITS FROM t^*

In Figure 16, we report the experiments for using 1 or 2 bits from t^* , which have not been used in all previously presented experiments. Recall the approximation in (6)

$$P[i_u^* = i_v^*] \approx P[(i_u^*, t_u^*) = (i_v^*, t_v^*)] = pGMM(u, v),$$

which, initially, was purely an empirical observation [25]. Characterizing this approximation for CWS remains an open problem. Figure 16 provides a validation study on M-Noise and M-Image, by adding the lowest 1 bit (dashed curve) or 2 bits (dashed dot curves) of t^* . We can see that adding 1 bit of t^* indeed helps slightly when we only use $b = 1$ or $b = 2$ bits for i^* . Using 2 bits for t^* does not lead further improvements. When we already use $b = 4$ or $b = 8$

Figure 15: GCWS with different p values, on the M-Noise1 dataset, for $b = 8$ and $k \in \{64, 512\}$. We can see that using $p \in [60, 150]$ produces the best results. The results of GCWSNet are still reasonable even with $p = 1$. Using the log-power transformation produces bad results except for p close to 1. Applying the power transformation directly on the original data produces pretty good results, which are still obviously worse than the results of GCWSNet.

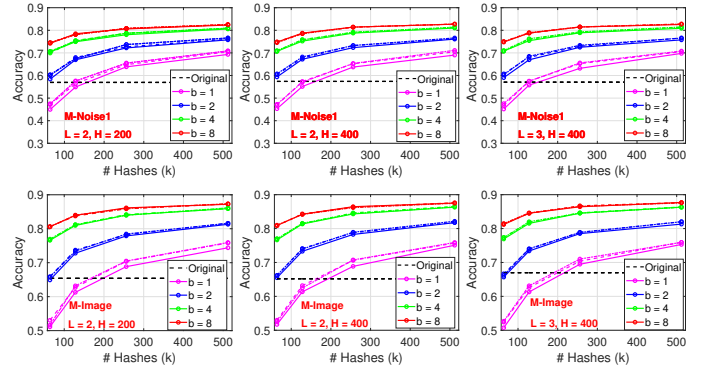


Figure 16: GCWSNet for M-Noise (with $p = 80$) and M-Image (with $p = 50$) by using 0 bit (solid), 1 bit (dashed), and 2 bits (dashed dot) for t^* in the output of GCWS hashing (i^*, t^*)

bits to encode i^* , then adding the information for 1 bit from t^* does not help in a noticeable manner.

We expect that practitioners would anyway use a sufficient number (e.g., 8) of bits for i^* . We therefore do not expect that using bits from t^* would help. Nevertheless, if it is affordable, we would suggest using the lowest 1 bit of t^* in addition to using b bits for i^* .

6 COMPARISON WITH NORMALIZED RANDOM FOURIER FEATURES (NRFF)

The method of random Fourier features (RFF) [35, 43, 44] is popular for approximating the RBF (Gaussian) kernel. For convenience, the

input data vectors are normalized to have unit l_2 norms, i.e., $\|u\| = \|v\| = 1$. The RBF (Gaussian) kernel is then $RBF(u, v; \gamma) = e^{-\gamma(1-\rho)}$, where $\rho = \rho(u, v) = \langle u, v \rangle$ is the cosine and $\gamma > 0$ is a tuning parameter. We sample $w \sim \text{uniform}(0, 2\pi)$, $r_i \sim N(0, 1)$ i.i.d., and denote $x = \sum_{i=1}^D u_i r_{ij}$, $y = \sum_{i=1}^D v_i r_{ij}$. Then we have $x \sim N(0, 1)$, $y \sim N(0, 1)$, and $E(\cos(\sqrt{\gamma}x + w) \cos(\sqrt{\gamma}y + w)) = e^{-\gamma(1-\rho)}$. The procedure is repeated k times to generate k RFF samples for each data vector. [26] advocated the so-called “normalized RFF” (NRFF) by normalizing the RFF’s to unit L2 norm, because the derived theoretical variance after normalizing becomes much smaller [26].

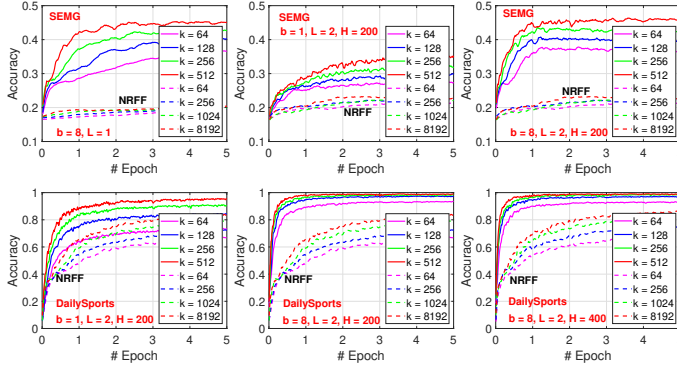


Figure 17: NRFF (dashed curves) versus GCWS (solid curves), for two datasets: SEMG and DailySports and $b \in \{1, 8\}$. We use much larger k values for NRFF, as large as 8192.

Figure 17 provides an experimental study to compare NRFF with GCWS on two datasets. While we still use $k \in \{64, 128, 256, 512\}$ for GCWS (solid curves), we have to present for k as large as 8192 for NRFF (dashed curves) because it is well-known that RFF needs a large number of samples in order to obtain reasonable results. It is quite obvious from Figure 17 that, at least on these two datasets, GCWS performs considerably better than NRFF at the same k (even if we just use $b = 1$ bit for GCWS). Also, we can see that GCWS converges much faster.

The method of random Fourier features is very popular in academic research. In comparison, research activities on consistent weighted sampling and variants are sparse. We hope this study might generate more interest in GCWS and motivate researchers as well as practitioners to try this interesting method.

7 APPLYING GCWS ON THE LAST LAYER OF TRAINED NETWORKS

We can always apply GCWS on the trained embedding vectors. Figure 18 illustrates such an example. We train a neural net on the original data with one hidden layer (i.e., $L = 2$) of $H \in \{200, 400\}$ hidden units. We directly apply GCWS on the output of the hidden layer and perform the classification task (i.e., a logistic regression) using the output of GCWS. We do this for every iteration of the neural net training process so that we can compare the entire history. From the plots, we can see that GCWS (solid red curves) can drastically improve the original test accuracy (dashed black curves), especially at the beginning of the training process, for example, improving the test accuracy from 20% to 70% after the first batch.

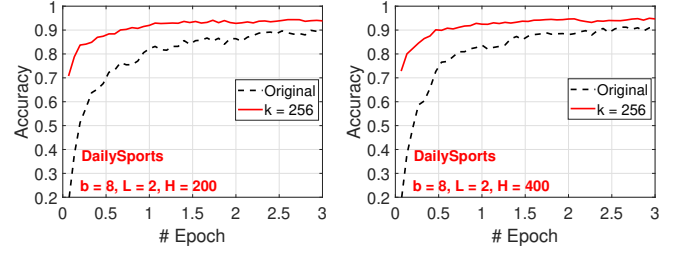


Figure 18: We apply GCWS ($k = 256$, $b = 8$) on the output of the last layer of neural net. For this case, the network has one hidden layer (i.e., $L = 2$) and $H \in \{200, 400\}$. We perform this operation at every batch, without affecting the accuracy of the original network, to obtain a history of improvements.

8 CONCLUDING REMARKS

In this paper, we adopt the pGMM kernel developed in 2017 [27] with a single tuning parameter p and use GCWS (generalized consistent weighted sampling) to generate hash values, producing sparse binary data vectors of size $2^b \times k$, where k is the number of hash samples and b is the number of bits to store each hash value. These binary vectors are fed to neural networks for subsequent tasks such as regression or classification. Our extensive experiments show that GCWS converges fast and typically reaches a reasonable accuracy at (less than) one epoch of training. This property of GCWS could be highly beneficial in practice because many important applications such as data streams or CTR predictions in commercial search engines typically train the models only with one epoch.

GCWS with a tuning parameter p provides a beneficial and robust power transformation on the original data. By adding this tuning parameter, the performance can often be improved, in some cases considerably so. Inside GCWS, this parameter acts on the (nonzero) data entry as $p \log u$. The nature of GCWS is that the coordinates of entries with larger values have a higher chance to be picked as output (in a probabilistic manner). In other words, both the absolute values and relative orders matter, and the power transformation does impact the performance. Experiments show that GCWSNet with a tuning parameter p produces more accurate results compared with two obvious strategies: 1) feeding power-transformed data (u^p) directly to neural nets; 2) feeding log-power-transformed data ($p \log u$, with zeros handled separately) directly to neural nets.

GCWSNet can be combined with count-sketch to reduce the model size of GCWSNet, which is proportional to $2^b \times k$ and can be pretty large if b is large such as 16 or 24. Our theoretical analysis for the impact of count-sketch on the estimation variance provides the explanation for the effectiveness of count-sketch demonstrated in the experiments. We recommend the “8-bit” practice in that we always use 2^8 bins for count-sketch if GCWS uses $b \geq 8$. With this strategy, even when $k = 2^{10} = 1024$, the model size is only proportional to $2^8 \times 2^{10} = 2^{18}$, which is not a large number.

There are other ways to take advantage of GCWS. For example, one can always apply GCWS on the embeddings of trained neural nets to hopefully boost the performance of existing network models. We also hope the comparison of GCWS with the popular random Fourier features would promote interest in future research.

REFERENCES

- [1] Michael Bendersky and W. Bruce Croft. Finding text reuse on the web. In *Proceedings of the Second International Conference on Web Search and Web Data Mining (WSDM)*, pages 262–271, Barcelona, Spain, 2009.
- [2] Léon Bottou, Olivier Chapelle, Dennis DeCoste, and Jason Weston, editors. *Large-Scale Kernel Machines*. The MIT Press, Cambridge, MA, 2007.
- [3] Andrei Z. Broder, Moses Charikar, Alan M. Frieze, and Michael Mitzenmacher. Min-wise independent permutations. In *Proceedings of the Thirtieth Annual ACM Symposium on the Theory of Computing (STOC)*, pages 327–336, Dallas, TX, 1998.
- [4] Andrei Z. Broder, Steven C. Glassman, Mark S. Manasse, and Geoffrey Zweig. Syntactic clustering of the web. *Comput. Networks*, 29(8-13):1157–1166, 1997.
- [5] Gregory Buehrer and Kumar Chellapilla. A scalable pattern mining approach to web graph compression with communities. In *Proceedings of the International Conference on Web Search and Web Data Mining (WSDM)*, pages 95–106, Stanford, CA, 2008.
- [6] Moses Charikar, Kevin Chen, and Martin Farach-Colton. Finding frequent items in data streams. *Theor. Comput. Sci.*, 312(1):3–15, 2004.
- [7] Moses S. Charikar. Similarity estimation techniques from rounding algorithms. In *Proceedings on 34th Annual ACM Symposium on Theory of Computing (STOC)*, pages 380–388, Montreal, Canada, 2002.
- [8] Ludmila Cherkasova, Kave Eshghi, Charles B. Morrey III, Joseph Tucek, and Alistair C. Veitch. Applying syntactic similarity algorithms for enterprise information management. In *Proceedings of the 15th ACM SIGKDD International Conference on Knowledge Discovery and Data Mining (KDD)*, pages 1087–1096, Paris, France, 2009.
- [9] Flavio Chierichetti, Ravi Kumar, Silvio Lattanzi, Michael Mitzenmacher, Alessandro Panconesi, and Prabhakar Raghavan. On compressing social networks. In *Proceedings of the 15th ACM SIGKDD International Conference on Knowledge Discovery and Data Mining (KDD)*, pages 219–228, Paris, France, 2009.
- [10] Yon Dourisboure, Filippo Geraci, and Marco Pellegrini. Extraction and classification of dense implicit communities in the web graph. *ACM Trans. Web*, 3(2):1–36, 2009.
- [11] Rong-En Fan, Kai-Wei Chang, Cho-Jui Hsieh, Xiang-Rui Wang, and Chih-Jen Lin. LIBLINEAR: A library for large linear classification. *J. Mach. Learn. Res.*, 9:1871–1874, 2008.
- [12] Hongliang Fei, Jingyuan Zhang, Xingxuan Zhou, Junhao Zhao, Xinyang Qi, and Ping Li. GemNN: Gating-enhanced multi-task neural networks with feature interaction learning for CTR prediction. In *Proceedings of the 44th International ACM SIGIR Conference on Research and Development in Information Retrieval (SIGIR)*, pages 2166–2171, Virtual Event, Canada, 2021.
- [13] Dennis Fetterly, Mark Manasse, Marc Najork, and Janet L. Wiener. A large-scale study of the evolution of web pages. In *Proceedings of the Twelfth International World Wide Web Conference (WWW)*, pages 669–678, Budapest, Hungary, 2003.
- [14] George Forman, Kave Eshghi, and Jaap Suermondt. Efficient detection of large-scale redundancy in enterprise file systems. *SIGOPS Oper. Syst. Rev.*, 43(1):84–91, 2009.
- [15] Min Fu, Dan Feng, Yu Hua, Xubin He, Zuoning Chen, Wen Xia, Yucheng Zhang, and Yujuan Tan. Design tradeoffs for data deduplication performance in backup workloads. In *Proceedings of the 13th USENIX Conference on File and Storage Technologies (FAST)*, pages 331–344, Santa Clara, CA, 2015.
- [16] Sreenivas Gollapudi and Rina Panigrahy. Exploiting asymmetry in hierarchical topic extraction. In *Proceedings of the 2006 ACM CIKM International Conference on Information and Knowledge Management (CIKM)*, pages 475–482, Arlington, VA, 2006.
- [17] Sreenivas Gollapudi and Aneesh Sharma. An axiomatic approach for result diversification. In *Proceedings of the 18th International Conference on World Wide Web (WWW)*, pages 381–390, Madrid, Spain, 2009.
- [18] Sergey Ioffe. Improved consistent sampling, weighted minhash and L1 sketching. In *Proceedings of the 10th IEEE International Conference on Data Mining (ICDM)*, pages 246–255, Sydney, Australia, 2010.
- [19] Nitin Jindal and Bing Liu. Opinion spam and analysis. In *Proceedings of the International Conference on Web Search and Web Data Mining (WSDM)*, pages 219–230, Palo Alto, CA, 2008.
- [20] Diederik P. Kingma and Jimmy Ba. Adam: A method for stochastic optimization. In *Proceedings of the 3rd International Conference on Learning Representations (ICLR)*, San Diego, CA, 2015.
- [21] Jon Kleinberg and Eva Tardos. Approximation algorithms for classification problems with pairwise relationships: Metric labeling and Markov random fields. In *Proceedings of the 40th Annual Symposium on Foundations of Computer Science (FOCS)*, pages 14–23, New York, NY, 1999.
- [22] Hugo Larochelle, Dumitru Erhan, Aaron C. Courville, James Bergstra, and Yoshua Bengio. An empirical evaluation of deep architectures on problems with many factors of variation. In *Proceedings of the Twenty-Fourth International Conference on Machine Learning (ICML)*, pages 473–480, Corvallis, OR, 2007.
- [23] Yifan Lei, Qiang Huang, Mohan S. Kankanhalli, and Anthony K. H. Tung. Locality-sensitive hashing scheme based on longest circular co-substring. In *Proceedings of the 2020 International Conference on Management of Data (SIGMOD)*, pages 2589–2599, Online conference [Portland, OR, USA], 2020.
- [24] Ping Li. Robust logitboost and adaptive base class (abc) logitboost. In *Proceedings of the Twenty-Sixth Conference Annual Conference on Uncertainty in Artificial Intelligence (UAI)*, pages 302–311, Catalina Island, CA, 2010.
- [25] Ping Li. 0-bit consistent weighted sampling. In *Proceedings of the 21th ACM SIGKDD International Conference on Knowledge Discovery and Data Mining (KDD)*, pages 665–674, Sydney, Australia, 2015.
- [26] Ping Li. Linearized GMM kernels and normalized random Fourier features. In *Proceedings of the 23rd ACM SIGKDD International Conference on Knowledge Discovery and Data Mining (KDD)*, pages 315–324, 2017.
- [27] Ping Li. Tunable GMM kernels. *arXiv preprint arXiv:1701.02046*, 2017.
- [28] Ping Li and Kenneth Ward Church. Using sketches to estimate associations. In *Proceedings of the Conference on Human Language Technology and the Conference on Empirical Methods in Natural Language Processing (HLT/EMNLP)*, pages 708–715, Vancouver, Canada, 2005.
- [29] Ping Li, Kenneth Ward Church, and Trevor Hastie. One sketch for all: Theory and application of conditional random sampling. In *Advances in Neural Information Processing Systems (NIPS)*, pages 953–960, Vancouver, Canada, 2008.
- [30] Ping Li and Arnd Christian König. b-bit minwise hashing. In *Proceedings of the 19th International Conference on World Wide Web (WWW)*, pages 671–680, Raleigh, NC, 2010.
- [31] Ping Li, Xiaoyun Li, Gennady Samorodnitsky, and Weijie Zhao. Consistent sampling through extremal process. In *Proceedings of the Web Conference (WWW)*, Virtual, 2021.
- [32] Ping Li, Xiaoyun Li, and Cun-Hui Zhang. Re-randomized densification for one permutation hashing and bin-wise consistent weighted sampling. In *Advances in Neural Information Processing Systems (NeurIPS)*, pages 15900–15910, Vancouver, Canada, 2019.
- [33] Ping Li, Anshumali Shrivastava, Joshua L. Moore, and Arnd Christian König. Hashing algorithms for large-scale learning. In *Advances in Neural Information Processing Systems (NIPS)*, pages 2672–2680, Granada, Spain, 2011.
- [34] Ping Li and Weijie Zhao. Fast ABC-Boost: A unified framework for selecting the base class in multi-class classification. *arXiv preprint arXiv:2205.10927*, 2022.
- [35] Xiaoyun Li and Ping Li. One-sketch-for-all: Non-linear random features from compressed linear measurements. In *Proceedings of the 24th International Conference on Artificial Intelligence and Statistics (AISTATS)*, pages 2647–2655, Virtual Event, 2021.
- [36] Xiaoyun Li and Ping Li. Rejection sampling for weighted jaccard similarity revisited. In *Proceedings of the Thirty-Fifth AAAI Conference on Artificial Intelligence (AAAI)*, Virtual Event, 2021.
- [37] Mark Manasse, Frank McSherry, and Kunal Talwar. Consistent weighted sampling. Technical Report MSR-TR-2010-73, Microsoft Research, 2010.
- [38] Emaad A. Manzoor, Sadeq M. Milajerdi, and Leman Akoglu. Fast memory-efficient anomaly detection in streaming heterogeneous graphs. In *Proceedings of the 22nd ACM SIGKDD International Conference on Knowledge Discovery and Data Mining (KDD)*, pages 1035–1044, San Francisco, CA, 2016.
- [39] Marc Najork, Sreenivas Gollapudi, and Rina Panigrahy. Less is more: sampling the neighborhood graph makes salsa better and faster. In *Proceedings of the Second International Conference on Web Search and Web Data Mining (WSDM)*, pages 242–251, Barcelona, Spain, 2009.
- [40] Sandeep Pandey, Andrei Broder, Flavio Chierichetti, Vanja Josifovski, Ravi Kumar, and Sergei Vassilvitskii. Nearest-neighbor caching for content-match applications. In *Proceedings of the 18th International Conference on World Wide Web (WWW)*, pages 441–450, Madrid, Spain, 2009.
- [41] Jannik Pevny, Behrad Garmany, Robert Gawlik, Christian Rossow, and Thorsten Holz. Cross-architecture bug search in binary executables. In *Proceedings of the 2015 IEEE Symposium on Security and Privacy (SP)*, pages 709–724, San Jose, CA, 2015.
- [42] Edward Raff and Charles K. Nicholas. An alternative to NCD for large sequences, lempel-ziv jaccard distance. In *Proceedings of the 23rd ACM SIGKDD International Conference on Knowledge Discovery and Data Mining (KDD)*, pages 1007–1015, Halifax, Canada, 2017.
- [43] Ali Rahimi and Benjamin Recht. Random features for large-scale kernel machines. In *Advances in Neural Information Processing Systems (NIPS)*, pages 1177–1184, Vancouver, Canada, 2007.
- [44] Walter Rudin. *Fourier Analysis on Groups*. John Wiley & Sons, New York, NY, 1990.
- [45] Erich Schubert, Michael Weiler, and Hans-Peter Kriegel. SigniTrend: scalable detection of emerging topics in textual streams by hashed significance thresholds. In *Proceedings of the 20th ACM SIGKDD International Conference on Knowledge Discovery and Data Mining (KDD)*, pages 871–880, New York, NY, 2014.
- [46] Anshumali Shrivastava. Simple and efficient weighted minwise hashing. In *Neural Information Processing Systems (NIPS)*, pages 1498–1506, Barcelona, Spain, 2016.
- [47] Anshumali Shrivastava and Ping Li. Fast near neighbor search in high-dimensional binary data. In *Proceedings of European Conference on Machine Learning and Knowledge Discovery in Databases (ECML-PKDD)*, pages 474–489, Bristol, UK, 2012.

- [48] Christopher Thomas and Adriana Kovashka. Preserving semantic neighborhoods for robust cross-modal retrieval. In *Proceedings of the 16th European Conference on Computer Vision (ECCV), Part XVIII*, pages 317–335, Glasgow, UK, 2020.
- [49] Kateryna Tymoshenko and Alessandro Moschitti. Cross-pair text representations for answer sentence selection. In *Proceedings of the 2018 Conference on Empirical Methods in Natural Language Processing (EMNLP)*, pages 2162–2173, Brussels, Belgium, 2018.
- [50] Tanguy Urvoy, Emmanuel Chauveau, Pascal Filoche, and Thomas Lavergne. Tracking web spam with html style similarities. *ACM Trans. Web*, 2(1):1–28, 2008.
- [51] Kilian Q. Weinberger, Anirban Dasgupta, John Langford, Alexander J. Smola, and Josh Attenberg. Feature hashing for large scale multitask learning. In *Proceedings of the 26th Annual International Conference on Machine Learning (ICML)*, pages 1113–1120, Montreal, Canada, 2009.
- [52] Qiang Yang and Xindong Wu. 10 challenging problems in data mining research. *International Journal of Information Technology & Decision Making*, 5(04):597–604, 2006.
- [53] Weijie Zhao, Deping Xie, Ronglai Jia, Yulei Qian, Ruiquan Ding, Mingming Sun, and Ping Li. Distributed hierarchical GPU parameter server for massive scale deep learning ads systems. In *Proceedings of Machine Learning and Systems 2020 (MLSys)*, Austin, TX, 2020.
- [54] Erkang Zhu, Dong Deng, Fatemeh Nargesian, and Renée J. Miller. JOSIE: overlap set similarity search for finding joinable tables in data lakes. In *Proceedings of the 2019 International Conference on Management of Data (SIGMOD)*, pages 847–864, Amsterdam, The Netherlands, 2019.